ACS Chemical Neuroscience

Letter

pubs.acs.org/chemneuro

Ca^{2+} Binding Protein S100A1 Competes with Calmodulin and PIP2 for Binding Site on the C-Terminus of the TPRV1 Receptor

Lenka Grycova,*[,†] Blanka Holendova,[†] Zdenek Lansky,[‡,∥] Ladislav Bumba,[§] Michaela Jirku,[†] Kristyna Bousova,[†] and Jan Teisinger*[,†]

[†]Institute of Physiology, [‡]Institute of Biotechnology, and [§]Institute of Microbiology, AS CR, v.v.i., Videnska 1083, 142 20 Prague 4, Czech Republic

[∥]B CUBE - Center for Molecular Bioengineering, Technische Universität Dresden, Arnoldstrasse 18, 01307 Dresden, Germany

ABSTRACT: Transient receptor potential vanilloid 1 ion channel (TRPV1) belongs to the TRP family of ion channels. These channels play a role in many important biological processes such as thermosensation and pain transduction. The TRPV1 channel was reported to be also involved in nociception. Ca^{2+} ions are described to participate in the regulation of TRP channels through the interaction with Ca^{2+}-binding proteins, such as calmodulin or S100A1. Calmodulin is involved in the Ca^{2+}-dependent regulation of TRPV1 via its binding to the TRPV1 C-terminal region. However, the role of the Ca^{2+}-binding protein S100A1 in the process of TRP channel regulation remains elusive. Here we characterized a region on the TRPV1 C-terminus responsible for the interaction with S100A1 using biochemical and biophysical tools. We found that this region overlaps with previously identified calmodulin and PIP2 binding sites and that S100A1 competes with calmodulin and PIP2 for this binding site. We identified several positively charged residues within this region, which have crucial impact on S100A1 binding, and we show that the reported S100A1−TRPV1 interaction is calcium-dependent. Taken together, our data suggest a mechanism for the mutual regulation of PIP2 and the Ca^{2+}-binding proteins S100A1 and calmodulin to TRPV1.

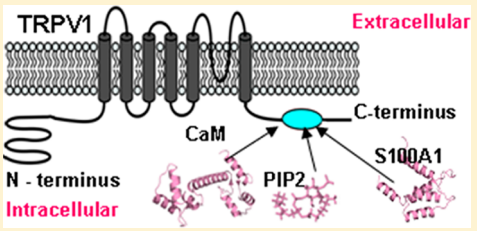

KEYWORDS: *TRPV1, vanilloid receptor, calmodulin, S100A1, calcium binding protein, surface plasmon resonance, fluorescence anisotropy*

The TRPV1 receptor is a member of the TRP channel family. This channel functions as a polymodal signal transducer of noxious stimuli. Recently, its predicted tetrameric structure and the membrane topology of its subunits have been confirmed: TRPV1 consists of six transmembrane helixes with a central pore region located between the fifth and the sixth transmembrane domain.[1] These structural features were verified by cryo-microscopy with sufficient resolution to reveal the principles of its gating mechanisms.[2] The intracellular termini contain important interaction sites for its agonists and regulatory molecules such as adenosine triphosphate (ATP), calmodulin, (CaM) and phosphatidyl inositol-4,5-bisphosphate (PIP2);[3−9] however, the structure of the intracellular regions has been solved only partially. The crystal structure of the isolated TRPV1 ankyrin repeat domain on the N-tail is the only known intracellular part.[3]

The activity of TRP channels is modulated by a wide range of stimuli. Usually the Ca^{2+} ions play an important role in these processes.[10] Calcium cellular level ranges from resting levels near 100 nM to signaling levels near 1 mM,[11] and regulates diverse amount of cellular processes through the interaction with a large number of calcium-sensor proteins such as CaM and S100A1. As reported previously, calcium takes part in the process of desensitizing TRPV1 receptors. This type of regulation is commonly tightly connected with Ca^{2+} binding proteins, such as CaM or S100A1 protein.[12] TRPV1 is inactivated via interactions with Ca^{2+}−CaM.[3,6,13] Similarly, Ca^{2+}-dependent cleavage of PIP2 and depletion of PIP2 is thought to play a major role in desensitization.[14−17] In contrast, the role of S100A1 in the process of TRP channel regulation remains elusive.

CaM is a small ubiquitously expressed protein, and its expression level ranges from nanomolar to micromolar levels.[18,19] Its structure in complex with various fragments derived from CaM-regulated proteins, both with and without Ca^{2+} ions (apocalmodulin), has been solved many times using NMR and X-ray diffraction. CaM has been described to interact with its targets in several ways. CaM contains four so-called EF hand motifs and undergoes large conformational changes upon Ca^{2+} binding. Two domains which participate in CaM binding in a Ca^{2+}-dependent manner have been identified within the intracellular termini of the TRPV1 receptor.[3,4] Nevertheless, the structure of TRPV1 in complex with CaM has not been determined yet.

S100 proteins are calcium-signaling molecules, which convert changes in cellular calcium levels to a variety of biological responses such as protein phosphorylation, cell growth and motility, cell-cycle regulation, transcription, differentiation and cell survival. S100A1 is one of the first proteins of this family to be characterized. It is a small (10.5 kDa) protein that forms

Published: December 29, 2014

DOI: 10.1021/cn500250r
ACS Chem. Neurosci. 2015, 6, 386−392

dimers. Along with CaM, S100A1 is a member of a large group of EF hand signaling proteins. CaM is present in all cells, and it is highly conserved among species. In contrast, S100 proteins are specific for vertebrates and have diverse tissue distributions.[20] S100A1 contains two EF-hand domains that bind Ca^{2+} ions with different affinities (500 μM and 1−50 μM),[21,22] and the S100A1 protein binds calcium and undergoes a conformational change by moving one helix and exposing a broad hydrophobic surface.[23] Several interactions of S100A1 protein with target molecules in Ca^{2+}dependent manner were described. Similarly to CaM, the dissociation constants of the S100A1 for its target range from nanomolar to micromolar levels.[24−26] Recently, some members of the TRP family were identified as biological targets of the S100 proteins. TRPV5 and TRPV6 interaction with the S100A10−annexin A2 complex is thought to mediate its trafficking to the plasma membrane.[27] Moreover, intracellular tails of TRPC6 and TRPM3 possess overlapping binding sites for S100A1 protein and CaM.[25,26] CaM and S100A1 also compete for binding sites within RyR1 receptor where they play a regulatory role.[22]

S100A1 and CaM have similar structural features, but no structural-functional studies or known physiological consequences of S100A1 binding to TRPV1 have been published yet. Here we utilize site-directed mutagenesis in combination with biophysical tools (steady-state fluorescence anisotropy, surface plasmon resonance (SPR)) to characterize the interaction of S100A1 with TRPV1. We show that S100A1 binds to TRPV1 and competes directly with CaM for the overlapping binding site on the C-terminus of TRPV1 (TRPV1-CT). Furthermore, we show that the interaction is calcium-dependent and that TRPV1 undergoes conformational changes upon binding to S100A1. In addition, we identified important basic residues of TRPV1 that actively participate in S100A1 binding.

RESULTS AND DISCUSSION

S100A1 Binds to TRPV1-CT. The C-terminus of TRPV1 contains a CaM binding site.[4,13,28] CaM typically recognizes motifs of hydrophobic and basic amino acid residues.[29] According to the CaM Target Database, the TRPV1-CT binding site has an atypical sequence but matches the so-called 1-8-14 conserved motif.[30] In previous reports, we found that the C-terminal region of TRPV1 (TRPV1-CT) harbors the integrative binding sites for CaM and PIP2.[4,31] Since a family of the Ca^{2+}-binding S100 proteins was shown to interact with similar binding motifs like CaM,[29,32] we sought to examine whether TRPV1-CT also shares binding site for the S100A1 protein. Ca^{2+} ions bind to two canonical EF hand motifs of S100A1 triggering a conformational switch of the S100A1 molecule and allowing the interaction between target protein and S100A1.[33] Hence, only the Ca^{2+}-bound conformation of S100A1 is able to recognize TRPV1 binding site. Thus, the experiments were done in Ca^{2+} excess to ensure only one population of S100A1 conformation occurs. First, steady-state fluorescence anisotropy measurements were employed to determine the role of Ca^{2+} in the interaction between TRPV1-CT and S100A1. As shown in Figure 1, titration of TRPV1-CT with fluorescently labeled S100A1 in the presence of 2 mM Ca^{2+} ions revealed an increase in fluorescence anisotropy indicating the formation of the TRPV1-CT/S100A1 complex with an estimated equilibrium dissociation constant of 169 ± 21 nM (mean ± SD, n = 3). In contrast, no changes in fluorescence anisotropy were observed during the titration experiments in the absence of Ca^{2+} ions suggesting that calcium

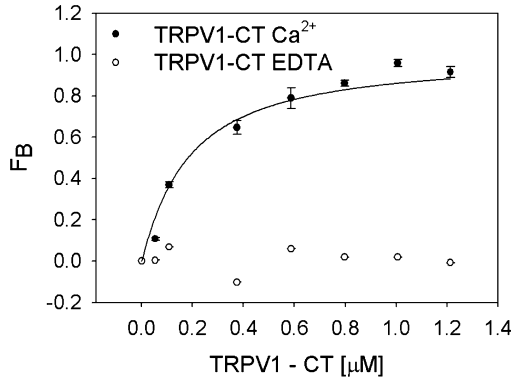

Figure 1. S100A1 binds TRPV1-CT in Ca^{2+}-dependent manner. Fluorescently labeled S100A1 was titrated with TRPV1-CT in the absence (○) and presence of 2 mM calcium ions (●), and the formation of the TRPV1-CT/S100A1 complex was followed by steady-state fluorescence anisotropy measurement. Fluorescence anisotropy was expressed as the bound fraction (FB) calculated according to eq 1 in the Methods. The solid line represents the binding isotherm determined by fitting the experimental data using a nonlinear least-squares analysis (see eq 2 in the Methods). The results are means ± SD from three independent experiments.

ions are strictly required for interaction between TRPV1-CT and S100A1. The kinetics of interaction between TRPV1-CT and S100A1 was further assessed by surface plasmon resonance (SPR). S100A1 was immobilized to a GLC chip at coupling level of 300 RU and washed in parallel by serially diluted TRPV1-CT at a flow rate of 30 μL/mL. Interaction of TRPV1-CT with S100A1 was specific, since negligible binding of thioredoxin alone was detected to the chip coated with S100A1 (Figure 2). Kinetic parameters of the interaction were calculated from global fitting of concentration-dependent binding curves (Figure 2A). The data were fitted to both a simple 1:1 Langmuir-type binding model and a conformational change model. We found that the interaction between S100A1 and TRPV1-CT is better described (in terms of reduced χ^2 and residual statistics) by the conformational change model indicating that formation of the complex occurs in two phases; a transient interaction of the TRPV1-CT and S100A1 subunits followed by a conformational transition of TRPV1-CT within the bound complex. Similar binding kinetics was also observed during the interaction of TRPV1-CT with CaM. As shown in Figure 2, the binding curves fit well to the conformational change model indicating that the formation of the TRPV1-CT/CaM complex is associated with a structural rearrangement of TRPV1-CT upon binding to CaM. The kinetic parameters of the interactions revealed that the rates of complex formation (represented here as association rate constants, k_{a1}) are similar for both S100A1 and CaM, but the stability of the complexes (represented by dissociation rate constant, k_{d1}) is significantly higher for S100A1. Thus, the binding affinity (K_{d1}) of TRPV1-CT to S100A1 is about two times higher for S100A1 than for CaM. (Table 1).

Alanine Scanning Mutagenesis of Basic Amino Acid Residues Engaged in Binding Site of TRPV1-CT. The importance of specific residues involved in binding of TRPV1-CT to CaM has been already investigated.[4,34] Based on the contact residues identified in the TRPV1-CT/CaM complex, alanine scanning mutagenesis of TRPV1-CT was performed followed by SPR analysis to assess the contribution of individual residues in kinetics of interaction and stability of

DOI: 10.1021/cn500250r
ACS Chem. Neurosci. 2015, 6, 386−392

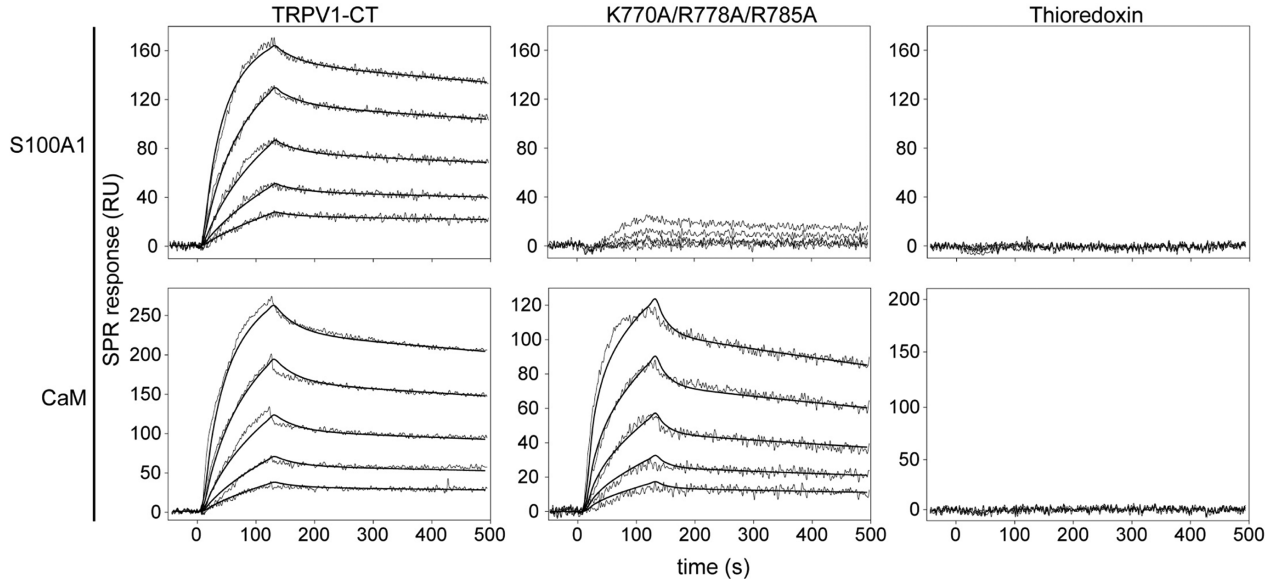

Figure 2. SPR kinetic binding analysis of the TRPV1-CT interaction with S100A1 and CaM. One-shot kinetics data of the wild-type TRPV1-CT (left column), the K770A/R778A/R785A mutant (middle column), and thioredoxin (right column) interacting with the Ca^{2+}-binding S100A1 protein (upper row) and CaM (lower row). The proteins were serially diluted (500, 250, 125, 62.5, and 31.25 nM) and injected in parallel over the sensor chip at flow rate of 30 μL/min. The kinetic data were globally fitted by using a conformational change model (see Methods). The fitted curves are superimposed as thin black line on top of the sensograms.

Table 1. Kinetic and Binding Affinity Constants for the Interactions of the C-Terminal Region of TRPV1 (TRPV1-CT) with the Ca^{2+}-Binding S100A1 Protein and Calmodulin (CaM)

		k_{a1} ($\times 10^4$ M^{-1} s^{-1})[a]	k_{d1} ($\times 10^{-2}$ s^{-1})[a]	K_{d1} ($\times 10^{-7}$ M)[ab]	k_{a2} ($\times 10^{-2}$ s^{-1})[a]	k_{d2} ($\times 10^{-4}$ s^{-1})[a]
WT	S100A	4.3 ± 0.8	0.7 ± 0.4	1.6 ± 0.4	1.5 ± 0.3	7.3 ± 0.9
	CaM	3.0 ± 0.4	12.3 ± 3.1	4.1 ± 0.9	1.7 ± 0.2	6.4 ± 0.2
K770A/R781A/R785A	S100A	4.7 ± 1.1	0.6 ± 0.2	1.3 ± 0.3	1.3 ± 0.4	7.4 ± 1.5
	CaM	2.0 ± 0.5	2.4 ± 0.5	1.2 ± 0.2	2.2 ± 0.3	5.1 ± 1.1
K770A/R785A	S100A	4.8 ± 1.1	1.8 ± 0.9	3.8 ± 0.3	1.3 ± 0.5	8.4 ± 2.1
	CaM	16.3 ± 0.5	1.5 ± 0.6	0.9 ± 0.4	1.9 ± 0.3	9.0 ± 1.0
K770A/R778A/R785A	S100A	ND	ND	ND	ND	ND
	CaM	4.2 ± 0.5	0.3 ± 0.1	0.7 ± 0.6	0.5 ± 0.3	3.1 ± 0.7
R771A/R781A	S100A	4.8 ± 0.5	8.8 ± 0.4	18.0 ± 0.6	1.1 ± 0.3	7.3 ± 0.5
	CaM	25.8 ± 2.5	0.9 ± 0.3	3.5 ± 0.8	1.1 ± 0.3	7.9 ± 3.8
R771A/R778A	S100A	2.2 ± 0.3	1.1 ± 0.7	5.0 ± 0.7	1.2 ± 0.4	7.6 ± 0. 5
	CaM	11.9 ± 2.4	1.9 ± 0.9	1.6 ± 0.4	1.7 ± 0.5	6.0 ± 1.2
R881A	S100A	1.5 ± 0.1	1.1 ± 0.4	7.3 ± 2.4	2.2 ± 0.3	4.3 ± 2.5
	CaM	5.3 ± 0.2	0.5 ± 0.2	0.9 ± 0.3	1.1 ± 0.3	5.1 ± 4.5

[a]The results are means ± SD from the SPR analysis of two independent experiments carried out in triplicate. [b]The equilibrium dissociation constant of the initial phase of the interaction, K_{d1}, was determined as k_{d1}/k_{a1}.

the TRPV1-CT/S100A1complex. Overall comparison of K_{d1} values revealed significant decrease in the binding affinity (increase in K_{d1}) for the TRPV1-CT mutants (Table 1). The predominant mechanism that contributed to the decreased binding affinity of the mutants to S100A1 was the faster dissociation rate of the encounter complex (represented by k_{d1}) indicating a lower stability of the complex as compared to the wild-type. On the other hand, a significant decrease in the association rates of the encounter complex (k_{a1}) was detected for the R771A/R778A and R881A mutations suggesting that the formation of the complex is also affected in these mutants. The mutation K770A/R781A/R785A did not affect the binding of TRPV1-CT to S100A1. The double mutation (K770A/R785A, R771A/R778A) and the single substitution (R881A) caused up to 5-fold decrease in the binding affinity, while the affinity of S100A1 for the R771A/R781A mutant was about 1 order of magnitude lower than for the wild-type. In contrast, the binding of the K770A/R778A/R785A triple mutant to S100A1 was completely inhibited indicating that these three residues play an important role in formation of the TRPV1-CT/S100A1 complex. The identical triple mutant has been previously shown to block interaction of TRPV1-CT with PIP2 embedded in the membrane of liposome.[31] However, the triple mutant K770/R778/R785 was still able to interact with CaM, even with a higher binding affinity than for the wild-type. It should be also emphasize that several TRPV1-CT mutants (namely K770A/R785A and R771A/R778A) had faster association rates (k_{a1}) for CaM resulting in higher tendency of these mutants to form the complexes with CaM. Such differences would be attributed to substantial divergences in the tertiary structures of S100A1 and CaM.[33] Taken together, these results showed that TRPV1-CT harbors the binding site for

DOI: 10.1021/cn500250r
ACS Chem. Neurosci. 2015, 6, 386−392

both S100A1 and CaM; however, the binding of S100A1 is more specific than that of CaM, which is likely to influence an intimate regulation of the TRPV1 channel.

S100A1 Competes with CaM and PIP2 for Binding to TRPV1-CT. In order to determine whether S100A1 competes with CaM for the same binding site on the TRPV1-CT, CaM was mixed with TRPV1-CT in a molar ratio of 1:1 and the capacity of the prepared TRPV1-CT/CaM complex to bind S100A1 was analyzed by using SPR. As shown in Figure 3, the

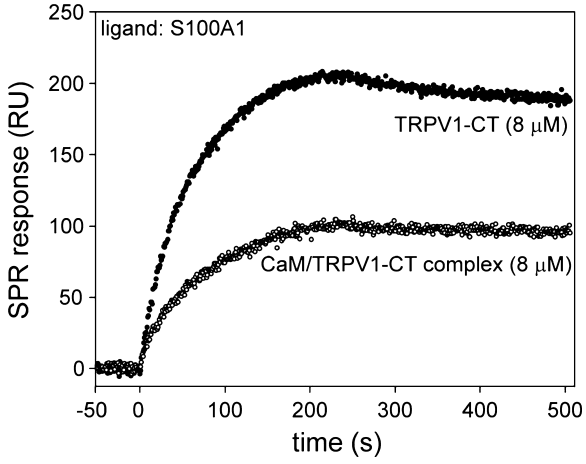

Figure 3. S100A1 and CaM share the binding site within the TRPV1-CT. TRPV1-CT (8 μM) and the TRPV1-CT/CaM complex (8 μM) were injected in parallel over the SPR sensor chip coated with S100A1 at flow rate of 30 μL/min. Inhibition of binding of the TRPV1-CT/CaM complex to S100A1 is represented by a decrease of SPR signal response.

binding of the TRPV1-CT/CaM complex was reduced to about 50% as compared to TRPV1-CT alone, indicating that S100A1 and CaM compete for the identical binding site within TRPV1-CT. In view of the fact that CaM shares the TRPV1-CT binding site with PIP2, we sought to examine whether S100A1 is also able to compete with PIP2 for binding to TRPV1-CT. The PIP2-enriched liposomes were immobilized to the sensor chip and the capacity of the preformed TRPV1-CT/S100A1 complex to interact with the membrane-bound PIP2 was probed by SPR. As shown in Figure 4A, the binding of the TRPV1-CT/S100A1 complex was almost completely inhibited as compared to TRPV1-CT alone suggesting that the binding site for S100A1 overlaps with the PIP2-binding site on TRPV1-CT. Reversely, only a very small portion (about 1/10) of the TRPV1-CT molecules attached to the PIP2-enriched liposomes were shown to interact with S100A1 (SPR response of 470 and 50 RU for TRPV1-CT and S100A1, respectively) indicating that S100A1 is not able to form a 1:1 complex with TRPV1-CT when bound to PIP2.(Figure 4B). Collectively, these data indicated that S100A1 competes with CaM and PIP2 for the binding site on TRPV1-CT.

TRPV1 is an important nociceptor. Regulation of its activity is proposed to be mediated via interactions with sensitizing agents as for example PIP2[3,14−17,35] or desensitizing agents as for example CaM.[3,4,6,13] Both of these ligands interact with the TRPV1-CT integrative binding site. We showed here that the third ligand, S100A1 protein, competes with CaM and PIP2 for identical binding site on TRPV1-CT and triggers the conformational changes of TRPV1 upon binding. The calcium sensor proteins CaM and S100A1 often interact with the same

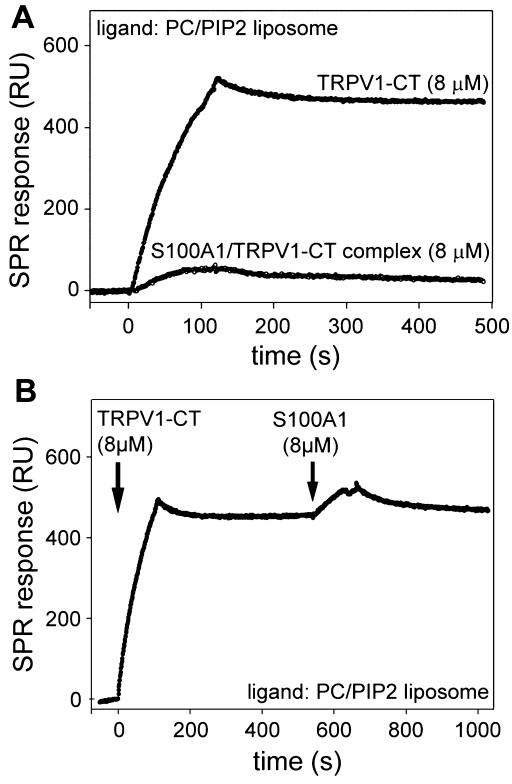

Figure 4. S100A1 and PIP2 share the binding site within the TRPV1-CT. (A) TRPV1-CT (8 μM) and the TRPV1-CT/S100A1 complex (8 μM) were injected in parallel over the SPR sensor chip coated with the PC/PIP2 (80:20) liposomes at flow rate of 30 μL/min. Inhibition of binding of the TRPV1-CT/S100A1 complex to the PIP2-enriched liposomes is represented by a decrease of SPR signal response. (B) SPR kinetic binding of S100A1 to TRPV1-CT bound to the PIP2-enriched liposome. TRPV1-CT (8 μM) was injected over the SPR sensor chip coated with PC/PIP2 (80:20) liposomes, left to dissociate, and immediately overlaid with subsequent injection of S100A1 (8 μM) onto the identical surface. The arrows represent injection of individual proteins. The flow rate was maintained at 30 mL/min during the whole experiment.

target proteins[22] and S100A has been shown to play a regulatory role.[36] While CaM participates in TRPV1 desensitization the physiological role of S1000A1 in TRPV1 activity modulation is elusive. The binding affinity of TRPV1-CT for S100A1 and CaM is comparable and ranges in submicromolar levels. Typical concentrations of S100A1 protein and CaM in the cell cytosol are estimated to be in a broad range (from nanomolar to micromolar levels),[37,38] but they are strictly tissue and cell specific. Whether the TRPV1/S100A1 interaction has a regulatory function thus remains to be tested as more electrophysiological information on S100 proteins in complex with TRP channels become available.

METHODS

TRPV1-CT Expression and Purification. The C-terminal part of rat TRPV1 (amino acids 712−838) (TRPV1-CT) was cloned into the bacterial expression vector pET32b (Novagen) as was described in detail previously.[31] Point mutations of several amino acid residues for alanine (R771A, R778A, K770A/R785A, R771A/R781A, R771A/R778A, K770A/R778A/R785A, K770A/R781A/R785A) were introduced by using PfuUltra high-fidelity DNA polymerase (Stratagene). The results of the mutagenesis were verified by sequencing. TRPV1-CT and all its mutant versions were expressed fused with the thioredoxin protein and a His-tag on the N-terminus in Rosetta

DOI: 10.1021/cn500250r
ACS Chem. Neurosci. 2015, 6, 386−392

Escherichia coli cells. The protein expression was induced by isopropyl 1-thio-β-D-galactopyranoside (Roth) for 12 h at 20 °C. Proteins were purified using Chelating Sepharose Fast Flow (GE Healthcare) according to the standard protocol followed by gel permeation chromatography on a Superdex 75 column (GE Healthcare). Protein concentration was assessed by measuring the absorption at 280 nm. The purity was verified using 12% SDS-polyacrylamide gel electrophoresis (PAGE).

S100A1 Cloning, Expression, Purification, and Labeling. cDNA coding for the human S100A1 protein was cloned into the pET28b expression vector. The protein was expressed in BL21 *E. coli* cells. Protein expression was induced by isopropyl-1-thio-β-D-galactopyranoside (Roth) for 12 h at 25 °C. The cells were pelleted by centrifugation and resuspended in 50 mM Tris-HCl buffer (pH 7.5) containing 2 mM EDTA and 0.2 mM PMSF. The cells were disrupted by sonication and centrifuged. $CaCl_2$ was added to the supernatant (final concentration 5 mM). The protein was purified using affinity chromatography on Phenyl Sepharose CL4B (Amersham Biosciences), where 50 mM Tris-HCl buffer (pH 7.5) containing 1.5 mM EDTA and 100 mM NaCl was used for the elution. Gel permeation chromatography on a Superdex 75 column (Amersham Pharmacia Biotech) was used as a final purification step. The protein was eluted with 50 mM HEPES buffer (pH 7.0) containing 250 mM NaCl, 2 mM $CaCl_2$, 2 mM β-mercaptoethanol, and 10% glycerol. Protein samples were concentrated using spin columns for protein concentration (Millipore). Protein concentration was assessed by measuring absorption at 280 nm. The purity was verified using 15% SDS-polyacrylamide gel electrophoresis (PAGE).

The protein was then dialyzed overnight into 10 mM NaHCO3 (pH 10.0) at 4 °C. For fluorescent labeling, S100A1 was mixed with 0.6 M dansyl chloride (DNS) solution (Sigma) at a molar ratio of 1:1.5 and incubated at room temperature for 8 h. The mixture was dialyzed overnight at 4 °C against 20 mM Tris-HCl buffer (pH 8.0) containing 250 mM NaCl and 2 mM $CaCl_2$ to remove the free DNS. The level of protein labeling was checked by measuring the ratio of the fluorescence intensities of the unbound and bound states (excitation at 340 nm, emission at 500 nm).

CaM Expression, Purification, and Labeling. CaM was expressed and purified according to the protocol published in our previous work.[39] The protein was labeled with the fluorescent probe DNS, as described above for S100A1.

Preparation of the TRPV1-CT/CaM and TRPV1-CT/S100A1 Complexes. The proteins were mixed with a 1:1 molar ratio and incubated for 1 h at room temperature in the presence of 2 mM Ca^{2+} followed by gel permeation chromatography on a Superdex 75 column (GE Healthcare). The freshly prepared complexes were immediately used for the binding experiments.

Steady State Fluorescence Anisotropy Binding Assay. Fluorescence anisotropy was measured in an ISS photon counting steady-state spectrofluorimeter (ISS PC1TM) at room temperature in a buffer containing 20 mM Tris-HCl (pH 7.5), 6 mM $CaCl_2$, and 2.66 mM DNS-S100A1. The final concentration of the fluorescently labeled protein in the measuring buffer in the cuvette was 10 nM. Increasing amounts of the solution of TRPV1-CT protein were titrated into the cuvette. DNS-S100A1 was excited at 340 nm, and fluorescence was collected at 500 nm. Steady-state fluorescence anisotropy was recorded at each protein concentration. The fraction of TRPV1-CT bound to the fluorescent probe, F_B, was determined from the anisotropy changes using eq 1:

$$F_B = \frac{(r_{obs} - r_{min})}{(r_{max} - r_{obs})Q + (r_{obs} - r_{min})} \quad (1)$$

where r_{min} and r_{max} are the anisotropies of the free and bound DNS-S100A1, respectively, r_{obs} is the observed anisotropy, and Q is the ratio of the fluorescence intensities of the free and bound protein (f_{max}/f_{min}).[40] All experiments were carried out at least in triplicate. F_B was plotted against TRPV1 protein concentration and fitted using equation

$$F_B = \frac{K_D + [P_1] + [P_2] - \sqrt{(K_D + [P_1] + [P_2])^2 - 4[P_1][P_2]}}{2[P_1]} \quad (2)$$

to determine the equilibrium dissociation constant (K_D) for TRPV1/S100A1 complex formation.[40] Nonlinear data fitting was performed using the package SigmaPlot 2000 (6.1) SPSS Inc. P_1 is the concentration of DNS-S100A1, and P_2 is the concentration of TRPV1 fusion protein.

Surface Plasmon Resonance (SPR). All SPR measurements were performed at 25 °C using CaM- and S100A1-coated GLC sensor chip mounted on a ProteOn XPR36 protein interaction array system (Bio-Rad, Hercules, CA). CaM and S100A1 proteins were diluted to a final concentrations of 10 μg/mL in 10 mM acetate buffer (pH 3.5) and washed over the sensor chip using a ProteOn amine coupling kit (Bio-Rad) at a flow rate of 30 μL/min followed by the injection of 1 M ethanolamine (pH 8.5) to block nonreacted groups. The subsequent SPR measurements were carried out in 10 mM HEPES (pH 7.4), 150 mM NaCl, 2 mM $CaCl_2$, and 0.005% Tween 20 at a flow rate of 30 μL/min. The proteins were serially diluted in running buffer to the indicated concentrations, and injected in parallel ("one-shot kinetics") over the CaM and S100A1 surface. Surfaces were typically regenerated with 100 μL of 50 mM EDTA, 1 M NaCl. The binding curves were processed by using a ProteOn Manager software (Bio-Rad) and corrected for sensor background by interspot referencing (the sites within the 6 × 6 array which are not exposed to ligand immobilization but are exposed to analyte flow), and double referenced by subtraction of analyte (channels 1−5) using a "blank" injection (channel 6). The data were analyzed globally by fitting both the association and the dissociation phases simultaneously for five different protein concentrations using both a 1:1 Langmuir-type binding model and the two-state (conformational change) model to determine the kinetics association and dissociation rate constants. The Langmuir-type model assumes the interaction between protein A and B resulting in a direct formation of the final complex (AB):

$$A + B \underset{k_d}{\overset{k_a}{\rightleftarrows}} AB$$

where k_a and k_d are the association and the dissociation rate constants, respectively. The two-state (conformational change) model assumes the two-step association process:

$$A + B \underset{k_{d1}}{\overset{k_{a1}}{\rightleftarrows}} [AB]^* \underset{k_{d2}}{\overset{k_{a2}}{\rightleftarrows}} AB$$

where [AB]* and AB represent encounter complex (transition state) and final docked state, respectively. Parameters k_{a1} and k_{d1} are the association and the dissociation rate constants for the first step (encounter complex formation), while k_{a2} and k_{d2} are forward and reverse rate constants for the second step (conformational change).

Interaction of TRPV1-CT and the TRPV1-CT/S100A1 complex with the PIP2-enriched liposomes was performed as previously described.[31] In brief, the liposomes (100 nm in diameter) made from 1,2-dimyristoyl-*sn*-glycero-3-phosphocholine (PC) and L-α-phosphatidylinositol-4,5-bisphosphate (PIP2) (Avanti Lipids, Alabaster, AL) were immobilized to a neutravidin-coated NLC chip (Biorad, Hercules, CA) using a pair of two complementary oligonucleotides, modified at their 5′ ends by biotin and cholesterol, respectively. The proteins were injected at identical concentrations (8 μM) at a flow rate of 30 μL/min.

AUTHOR INFORMATION

Corresponding Authors

*E-mail: l.grycova@biomed.cas.cz.

*E-mail: teisingr@biomed.cas.cz.

Author Contributions

L.G. designed the experiments, performed the experiments, analyzed the data, contributed reagents/materials/analysis

DOI: 10.1021/cn500250r
ACS Chem. Neurosci. 2015, 6, 386−392

tools, and wrote the paper. B.H. performed the experiments and wrote the paper. Z.L. analyzed the data, contributed reagents/materials/analysis tools, and wrote the paper. L.B. designed the experiments, performed the experiments, analyzed the data, and wrote paper. M.J. and K.B. performed the experiments. J.T. designed the experiments, contributed reagents/materials/analysis tools, and wrote the paper.

Funding

This study was supported by the Grant Agency of the Czech Republic (Grant Nos. 301/10/1159, 207/11/0717, 15-11851S), Grant Agency of Charles University (842314, 238214), the Grant Agency of the Czech Republic Project of Excellence in the Field of Neuroscience (P304/12/G069), BIOCEV CZ.1.05/1.1.00/02.0109 from the ERDF and by institutional support by RVO 86 652 036.

Notes

The authors declare no competing financial interest.

REFERENCES

(1) Liao, M., Cao, E., Julius, D., and Cheng, Y. (2013) Structure of the TRPV1 ion channel determined by electron cryo-microscopy. *Nature 504*, 107−112.

(2) Cao, E., Liao, M., Cheng, Y., and Julius, D. (2013) TRPV1 structures in distinct conformations reveal activation mechanisms. *Nature 504*, 113−118.

(3) Lishko, P. V., Procko, E., Jin, X., Phelps, C. B., and Gaudet, R. (2007) The ankyrin repeats of TRPV1 bind multiple ligands and modulate channel sensitivity. *Neuron 54*, 905−918.

(4) Grycova, L., Lansky, Z., Friedlova, E., Obsilova, V., Janouskova, H., Obsil, T., and Teisinger, J. (2008) Ionic interactions are essential for TRPV1 C-terminus binding to calmodulin. *Biochem. Biophys. Res. Commun. 375*, 680−683.

(5) Brauchi, S., Orta, G., Mascayano, C., Salazar, M., Raddatz, N., Urbina, H., Rosenmann, E., Gonzalez-Nilo, F., and Latorre, R. (2007) Dissection of the components for PIP2 activation and thermosensation in TRP channels. *Proc. Natl. Acad. Sci. U. S. A. 104*, 10246−10251.

(6) Rosenbaum, T., Gordon-Shaag, A., Munari, M., and Gordon, S. E. (2004) Ca^{2+}/calmodulin modulates TRPV1 activation by capsaicin. *J. Gen. Physiol. 123*, 53−62.

(7) Prescott, E. D., and Julius, D. (2003) A modular PIP2 binding site as a determinant of capsaicin receptor sensitivity. *Science 300*, 1284−1288.

(8) Zhu, M. X. (2005) Multiple roles of calmodulin and other Ca^{2+}-binding proteins in the functional regulation of TRP channels. *Pfluegers Arch. 451*, 105−115.

(9) Grycova, L., Lansky, Z., Friedlova, E., Vlachova, V., Kubala, M., Obsilova, V., Obsil, T., and Teisinger, J. (2007) ATP binding site on the C-terminus of the vanilloid receptor. *Arch. Biochem. Biophys. 465*, 389−398.

(10) Pedersen, S. F., Owsianik, G., and Nilius, B. (2005) TRP channels: An overview. *Cell Calcium 38*, 233−252.

(11) Yamniuk, A. P., and Vogel, H. J. (2004) Calmodulin's flexibility allows for promiscuity in its interactions with target proteins and peptides. *Mol. Biotechnol. 27*, 33−57.

(12) Vetter, S. W., and Leclerc, E. (2003) Novel aspects of calmodulin target recognition and activation. *Eur. J. Biochem. 270*, 404−414.

(13) Numazaki, M., Tominaga, T., Takeuchi, K., Murayama, N., Toyooka, H., and Tominaga, M. (2003) Structural determinant of TRPV1 desensitization interacts with calmodulin. *Proc. Natl. Acad. Sci. U. S. A. 100*, 8002−8006.

(14) Liu, B., Zhang, C., and Qin, F. (2005) Functional recovery from desensitization of vanilloid receptor TRPV1 requires resynthesis of phosphatidylinositol 4,5-bisphosphate. *J. Neurosci. 25*, 4835−4843.

(15) Lukacs, V., Thyagarajan, B., Varnai, P., Balla, A., Balla, T., and Rohacs, T. (2007) Dual regulation of TRPV1 by phosphoinositides. *J. Neurosci. 27*, 7070−7080.

(16) Mercado, J., Gordon-Shaag, A., Zagotta, W. N., and Gordon, S. E. (2010) Ca^{2+}-dependent desensitization of TRPV2 channels is mediated by hydrolysis of phosphatidylinositol 4,5-bisphosphate. *J. Neurosci. 30*, 13338−13347.

(17) Stein, A. T., Ufret-Vincenty, C. A., Hua, L., Santana, L. F., and Gordon, S. E. (2006) Phosphoinositide 3-kinase binds to TRPV1 and mediates NGF-stimulated TRPV1 trafficking to the plasma membrane. *J. Gen. Physiol. 128*, 509−522.

(18) Tran, Q. K., Black, D. J., and Persechini, A. (2003) Intracellular coupling via limiting calmodulin. *J. Biol. Chem. 278*, 24247−24250.

(19) Burgoyne, R. D., and Haynes, L. P. (2010) Neuronal calcium sensor proteins: Emerging roles in membrane traffic and synaptic plasticity. *F1000 Biol. Rep. 2*, 5 DOI: 10.3410/B2-5.

(20) Kato, K., Kimura, S., Haimoto, H., and Suzuki, F. (1986) S100a0 (alpha alpha) protein: Distribution in muscle tissues of various animals and purification from human pectoral muscle. *J. Neurochem. 46*, 1555−1560.

(21) Rustandi, R. R., Baldisseri, D. M., Inman, K. G., Nizner, P., Hamilton, S. M., Landar, A., Zimmer, D. B., and Weber, D. J. (2002) Three-dimensional solution structure of the calcium-signaling protein apo-S100A1 as determined by NMR. *Biochemistry 41*, 788−796.

(22) Wright, N. T., Prosser, B. L., Varney, K. M., Zimmer, D. B., Schneider, M. F., and Weber, D. J. (2008) S100A1 and calmodulin compete for the same binding site on ryanodine receptor. *J. Biol. Chem. 283*, 26676−26683.

(23) Rezvanpour, A., and Shaw, G. S. (2009) Unique S100 target protein interactions. *Gen. Physiol. Biophys. 28*, F39−46.

(24) Treves, S., Scutari, E., Robert, M., Groh, S., Ottolia, M., Prestipino, G., Ronjat, M., and Zorzato, F. (1997) Interaction of S100A1 with the Ca^{2+} release channel (ryanodine receptor) of skeletal muscle. *Biochemistry 36*, 11496−11503.

(25) Bily, J., Grycova, L., Holendova, B., Jirku, M., Janouskova, H., Bousova, K., and Teisinger, J. (2013) Characterization of the S100A1 protein binding site on TRPC6 C-terminus. *PLoS One 8*, e62677.

(26) Holakovska, B., Grycova, L., Jirku, M., Sulc, M., Bumba, L., and Teisinger, J. (2012) Calmodulin and S100A1 protein interact with N terminus of TRPM3 channel. *J. Biol. Chem. 287*, 16645−16655.

(27) van de Graaf, S. F., Hoenderop, J. G., Gkika, D., Lamers, D., Prenen, J., Rescher, U., Gerke, V., Staub, O., Nilius, B., and Bindels, R. J. (2003) Functional expression of the epithelial Ca^{2+} channels (TRPV5 and TRPV6) requires association of the S100A10-annexin 2 complex. *EMBO J. 22*, 1478−1487.

(28) Lau, S. Y., Procko, E., and Gaudet, R. (2012) Distinct properties of Ca^{2+}-calmodulin binding to N- and C-terminal regulatory regions of the TRPV1 channel. *J. Gen Physiol 140*, 541−555.

(29) Rhoads, A. R., and Friedberg, F. (1997) Sequence motifs for calmodulin recognition. *FASEB J. 11*, 331−340.

(30) Yap, K. L., Kim, J., Truong, K., Sherman, M., Yuan, T., and Ikura, M. (2000) Calmodulin target database. *J. Struct. Funct. Genomics 1*, 8−14.

(31) Grycova, L., Holendova, B., Bumba, L., Bily, J., Jirku, M., Lansky, Z., and Teisinger, J. (2012) Integrative binding sites within intracellular termini of TRPV1 receptor. *PLoS One 7*, e48437.

(32) Wilder, P. T., Lin, J., Bair, C. L., Charpentier, T. H., Yang, D., Liriano, M., Varney, K. M., Lee, A., Oppenheim, A. B., Adhya, S., Carrier, F., and Weber, D. J. (2006) Recognition of the tumor suppressor protein p53 and other protein targets by the calcium-binding protein S100B. *Biochim. Biophys. Acta 1763*, 1284−1297.

(33) Bhattacharya, S., Bunick, C. G., and Chazin, W. J. (2004) Target selectivity in EF-hand calcium binding proteins. *Biochim. Biophys. Acta 1742*, 69−79.

(34) Lau, S. Y., Procko, E., and Gaudet, R. (2012) Distinct properties of Ca^{2+}-calmodulin binding to N- and C-terminal regulatory regions of the TRPV1 channel. *J. Gen. Physiol. 140*, 541−555.

(35) Yao, J., and Qin, F. (2009) Interaction with phosphoinositides confers adaptation onto the TRPV1 pain receptor. *PLoS Biol. 7*, e46.

(36) Prosser, B. L., Hernandez-Ochoa, E. O., and Schneider, M. F. (2011) S100A1 and calmodulin regulation of ryanodine receptor in striated muscle. *Cell Calcium 50*, 323−331.

DOI: 10.1021/cn500250r
ACS Chem. Neurosci. 2015, 6, 386−392

(37) Su, A. I., Wiltshire, T., Batalov, S., Lapp, H., Ching, K. A., Block, D., Zhang, J., Soden, R., Hayakawa, M., Kreiman, G., Cooke, M. P., Walker, J. R., and Hogenesch, J. B. (2004) A gene atlas of the mouse and human protein-encoding transcriptomes. *Proc. Natl. Acad. Sci. U. S. A. 101*, 6062−6067.
(38) Chin, D., and Means, A. R. (2000) Calmodulin: a prototypical calcium sensor. *Trends Cell Biol. 10*, 322−328.
(39) Holakovska, B., Grycova, L., Bily, J., and Teisinger, J. (2011) Characterization of calmodulin binding domains in TRPV2 and TRPV5 C-tails. *Amino Acids 40*, 741−748.
(40) Lakowicz, J. r. (2006) *Principles of fluorescence spectroscopy*, 3rd ed., Springer, New York.

DOI: 10.1021/cn500250r
ACS Chem. Neurosci. 2015, 6, 386−392